An Extended-Gate Field-Effect Transistor With Low-Temperature Hydrothermally Synthesized SnO_2 Nanorods as pH Sensor

Hung-Hsien Li, Wei-Syuan Dai, Jung-Chuan Chou, and Huang-Chung Cheng, *Member, IEEE*

***Abstract*—An extended-gate field-effect transistor (EGFET) with low-temperature hydrothermally synthesized SnO_2 nanorods as the pH sensor was demonstrated for the first time. The SnO_2 nanorod sensor exhibited the higher sensitivity of 55.18 mV/pH and larger linearity of 0.9952 in the wide sensing range of pH 1–13 with respect to the thin-film one. The nearly 15% sensitivity enhancement for such a sensor was attributed to the high surface-to-volume ratio of the nanorod structure, reflecting larger effective sensing areas. The characteristics of the output voltage versus sensing time also indicated good reliability and durability for the SnO_2 nanorod sensor. Furthermore, the hysteresis was only 3.69 mV after the solution was changed as pH7 → pH3 → pH7 → pH11 → pH7.**

***Index Terms*—Extended-gate field-effect transistor (EGFET), hydrothermal method, pH sensor, SnO_2 nanorods.**

I. Introduction

In 1970, Bergveld proposed the ion-sensitive field-effect transistor (ISFET) in neurophysiological measurement [1]. The extended-gate field-effect transistor (EGFET) was introduced as an alternate for the fabrication of the ISFET by Van Der Spiegel *et al.* in 1983 [2]. In 2000, the separative structure of the EGFET with a commercial MOSFET was presented [3]. This structure had many advantages over the conventional ISFET, such as low cost, simpler packaging, temperature and light insensitivity, and better long-term stability [4], [5]. Distinguishing from the ISFET, oxide-based sensing films such as zinc oxide (ZnO) [6], tin oxide (SnO_2) [7], titanium oxide (TiO_2) [8], ruthenium oxide (RuO_2) [9], and vanadium oxide (V_2O_5) [10] were used for the sensing membranes of the EGFET. The reported methods, including sputtering and sol–gel, required vacuum facilities and high-temperature processes that limited the flexible substrate disposal.

Based on the site-binding model [11], the chemical sensitivity was dependent on the total number of surface sites per unit area (N_S). It suggested that the larger N_S would facilitate the ions sensing. Consequently, 1-D nanostructures such as nanowires, nanobelts, nanorods, and nanotubes had attracted a lot of attention for the pH sensing due to their high surface-to-volume ratio with larger effective sensing areas [12]–[14].

In this letter, a simple and low-temperature hydrothermal method was proposed to fabricate a SnO_2 nanorod sensor. The dense SnO_2 nanorods provided more surface sites for H^+ sensing. Our results demonstrated superior sensitivity, better linearity, and larger sensing range than the other nanostructure pH sensors [13]–[16]. It revealed the potential applications in pH sensing using SnO_2 nanorods.

II. Device Fabrication

Well-defined crystalline SnO_2 nanorods were synthesized on the polycrystalline fluorine-doped tin oxide (FTO) glass substrates via a hydrothermal method. The precursor solution was prepared by mixing 0.034-g tin (IV) chloride pentahydrate $(SnCl_4 \cdot 5H_2O)$ and 0.92-g urea $((NH_2)_2CO)$ in 100-mL deionized water. Then, the 5-mL HCl (37%) was added to adjust the pH value in this aqueous solution. After the solution was stirred for 10 min, the SnO_2 nanorods were grown on the FTO glass substrates at 95 °C in a quartz beaker placed in a kettle. The growth time was controlled as 48 h. Finally, the FTO glass substrate was removed from the solution, rinsed with deionized water, and then dried. For comparison, the SnO_2 thin film was also hydrothermally synthesized but with the $SnCl_4 \cdot 5H_2O$ weight of 0.34 g and the growth time of 24 h.

After the SnO_2 nanorods growth, the silver paste served as the electrode was applied to the FTO glass substrate. The metal wire was bound with silver paste and packaged with epoxy resin. Subsequently, the packaged electrode was dried in an oven at 120 °C for 30 min. Epoxy resin was used to define the sensing window of 2×2 mm^2. The SnO_2 sensing membrane and the reference electrode (Ag/AgCl) were then immersed in the different pH solutions and connected to the commercial standard MOSFET device (CD4007UB). The drift effects and hysteresis characteristics were measured using a commercial instrumentation amplifier (IC LT1167) and a digital multimeter (HP 34401A). All measurements were carried out in a dark box at room temperature in order to avoid the light and temperature interferences.

III. Results and Discussion

Fig. 1(a) and (b) exhibits the top view and 45°-tilted field-emission scanning electron microscopy (FE-SEM) images of the as-synthesized SnO_2 nanorods. Well-defined crystalline nanorods with a square structure are observed over the entire substrate. The average diameter and wire length of the SnO_2

Manuscript received June 29, 2012; accepted July 21, 2012. Date of publication August 31, 2012; date of current version September 21, 2012. This work was supported by the National Science Council of Taiwan under Grant NSC 99-2221-E-009-168-MY3. The review of this letter was arranged by Editor A. Nathan.

H.-H. Li, W.-S. Dai, and H.-C. Cheng are with the Department of Electronics Engineering and the Institute of Electronics, National Chiao Tung University, Hsinchu 30010, Taiwan (e-mail: et248854.ee97g@nctu.edu.tw).

J.-C. Chou is with the Graduate School of Electronic Engineering, National Yunlin University of Science and Technology, Yunlin 64002, Taiwan.

Color versions of one or more of the figures in this letter are available online at http://ieeexplore.ieee.org.

Digital Object Identifier 10.1109/LED.2012.2210274

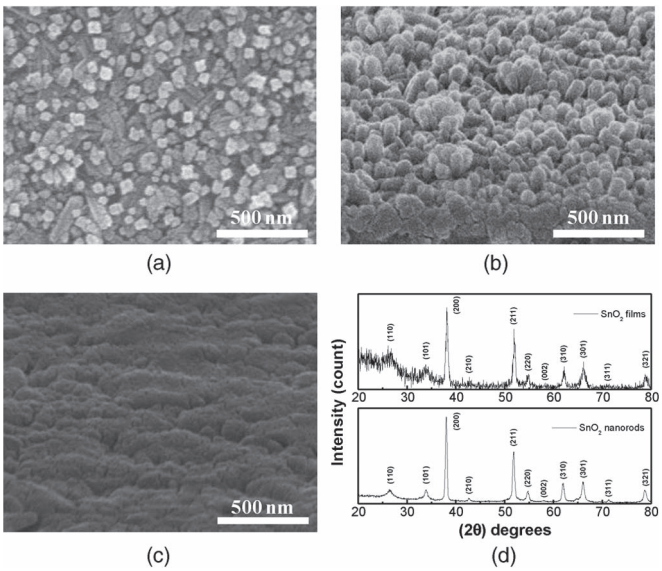

Fig. 1. (a) Top view and (b) 45°-tilted SEM images of the SnO_2 nanorods. (c) 45°-tilted SEM images of the SnO_2 films. (d) GAXRD peaks of the SnO_2 films and SnO_2 nanorods.

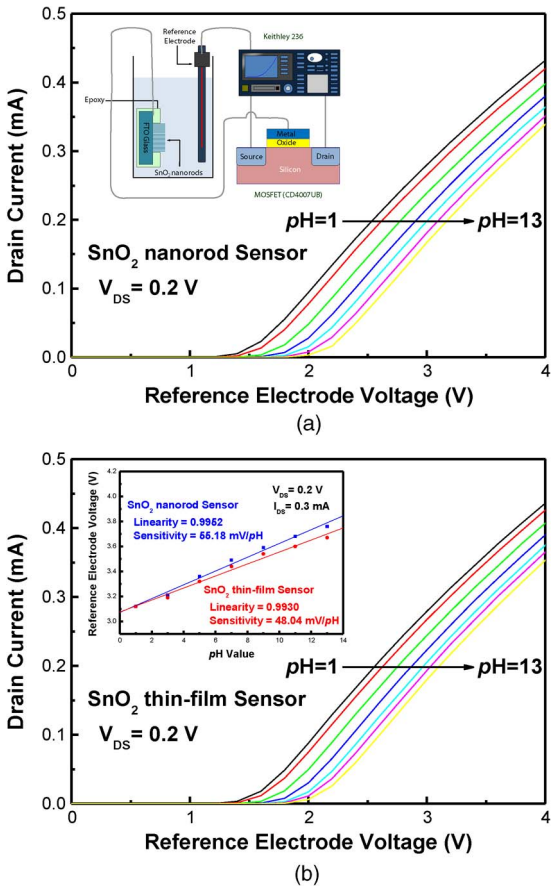

Fig. 2. (a) $I_{DS}-V_{\mathrm{REF}}$ measurements of the SnO_2 nanorod sensor and a schematic (inset) of the measurement layout. (b) $I_{DS}-V_{\mathrm{REF}}$ measurements of the SnO_2 thin-film sensor. Sensitivities and linearities (inset) of the SnO_2 nanorod and thin-film sensors in the linear region.

nanorods are around 50 and 150 nm, correspondingly. The 45°-tilted SEM image of the SnO_2 films is shown in Fig. 1(c). The glancing-angle X-ray diffractions (GAXRDs) of the SnO_2 films and SnO_2 nanorods are shown in Fig. 1(d). The SnO_2 nanorods

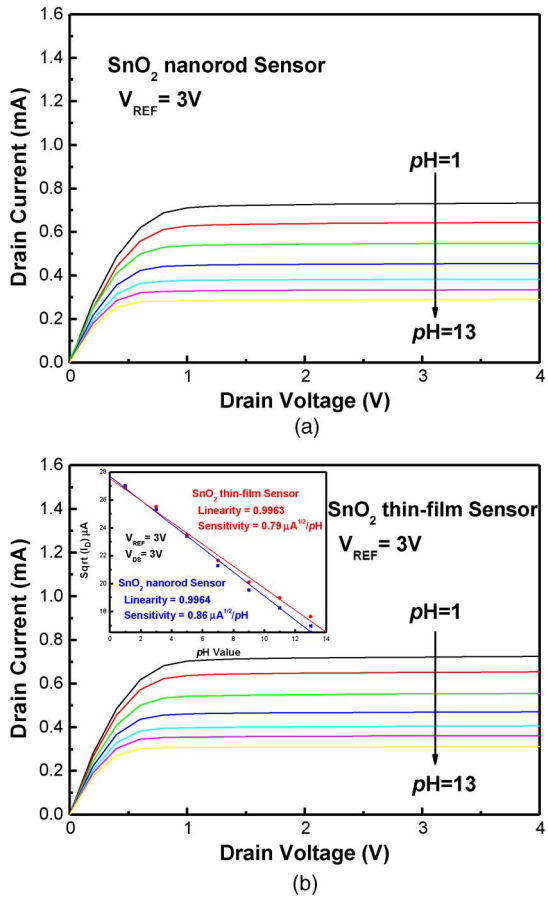

Fig. 3. (a) $I_{DS}-V_{DS}$ measurements of the SnO_2 nanorod sensor. (b) $I_{DS}-V_{DS}$ measurements of the SnO_2 thin-film sensor. Sensitivities and linearities (inset) of the SnO_2 nanorod and thin-film sensors in the saturation region.

are rutile (tetragonal crystal system) with the lattice constants of $a = 4.737$ Å and $c = 3.186$ Å. It is consistent with the square structure for the FE-SEM observation. The GAXRD peaks also reveal that the low-temperature hydrothermally synthesized SnO_2 films and SnO_2 nanorods are polycrystalline. The SnO_2 films show worse crystralline than the SnO_2 nanorods, implying more defects in the SnO_2 films.

The relation between the drain–source current (I_{DS}) and the pH value could be obtained using the basic MOSFET expression [17]. The transfer characteristics $(I_{DS}-V_{\mathrm{REF}})$ of the SnO_2 nanorod and thin-film sensors in the linear region (for V_{DS} fixed at 0.2 V, whereas V_{REF} scanned from 0 to 4 V) from pH1 to pH13 are shown in Fig. 2. It is observed that the threshold voltage shift depends upon the pH value. A schematic measurement layout is shown in the inset of Fig. 2(a). Fig. 2(b) (inset) illustrates the sensitivities and linearities of the SnO_2 nanorod and thin-film sensors. The results indicate that V_{REF} linearly depends on the pH value in the linear region (for I_{DS} fixed at 0.2 mA). The sensitivity and linearity of the SnO_2 nanorod sensor are 55.18 mV/pH and 0.9952, respectively. In contrast, the sensitivity and linearity of the thin-film one are 48.04 mV/pH and 0.9930, accordingly.

The output characteristics $(I_{DS}-V_{DS})$ of the SnO_2 nanorod and thin-film (inset) sensors in the saturation region (for V_{REF} fixed at 3 V, whereas V_{DS} scanned from 0 to 4 V) from pH1 to pH13 are shown in Fig. 3. It is observed that the drain

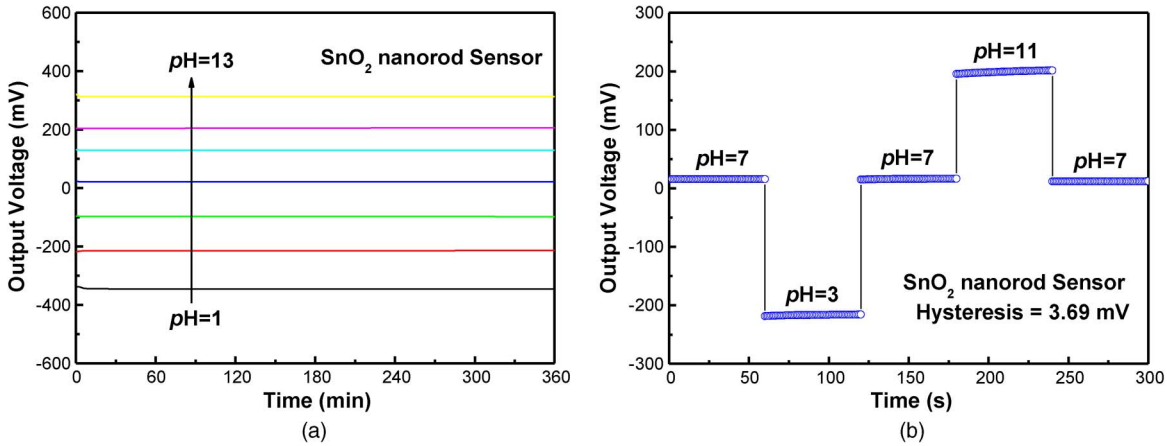

Fig. 4. (a) V–t curves and (b) hysteresis characteristics of the SnO_2 nanorod sensor.

current decreases with increasing the pH value. Fig. 3(b) (inset) indicates the sensitivities and linearities of the SnO_2 nanorod and thin-film sensors. The results indicate that $\sqrt{I_{DS}}$ linearly depends on the pH value in the saturation region (for V_{DS} fixed at 3 V). The sensitivity and linearity of the SnO_2 nanorod sensor are 0.86 $mA^{1/2}/pH$ and 0.9964, respectively. However, the sensitivity and linearity of the thin-film one are 0.79 $mA^{1/2}/pH$ and 0.9963 correspondingly.

Consequently, the SnO_2 nanorod sensor demonstrated the better sensitivity and superior linearity as compared with the thin-film one. It was attributed to the high surface-to-volume ratio for the nanorod structure to provide more surface sites and larger effective sensing areas.

The drift effect has been also used to estimate the reliability and durability of electrochemical sensors. Fig. 4(a) reveals the output voltage and sensing time $(V$–$t)$ characteristics of the SnO_2 nanorod sensor for 360-min duration. The output voltage increases with increasing the pH value. It demonstrated the good reliability and durability of the SnO_2 nanorod sensor. Fig. 4(b) displays the hysteresis characteristics of the SnO_2 nanorod sensor. The output offset voltage was measured for the 1-min interval between different pH solutions. The result indicated that the hysteresis is only 3.69 mV after the solution changes as pH7 $\rightarrow$ pH3 $\rightarrow$ pH7 $\rightarrow$ pH11 $\rightarrow$ pH7.

IV. Conclusion

A low-temperature hydrothermally synthesized SnO_2 nanorod EGFET as pH sensor has been proposed to achieve superior pH sensing characteristics as compared with the thin-film one in the wide sensing range of pH 1–13. It demonstrated that the SnO_2 nanorod sensor exhibited the higher sensitivity of 55.18 mV/pH and larger linearity of 0.9952 in the linear region. Furthermore, it also showed a better sensitivity of 0.86 $mA^{1/2}/pH$ and a greater linearity of 0.9964 in the saturation region. It was attributed to the high surface-to-volume ratio of the nanorod structure to provide more surface sites and oxygen vacancies, implying larger effective sensing areas. No obvious degradation for the $V - t$ measurement indicated that the SnO_2 nanorod sensor had good reliability and durability. Moreover, the hysteresis was only 3.69 mV after the solution was changed as pH7 $\rightarrow$ pH3 $\rightarrow$ pH7 $\rightarrow$ pH11 $\rightarrow$ pH7. Such low-temperature-fabricated SnO_2 nanorods with superior pH sensing characteristics revealed the potential applications in the flexible and disposable biosensors.

References

[1] P. Bergveld, "Development of an ion sensitive solid-state device for neurophysiological measurement," *IEEE Trans. Biomed. Eng.*, vol. BME-17, no. 1, pp. 70–71, Jan. 1970.

[2] J. Van Der Spiegel, I. Lauks, P. Chan, and D. Babic, "The extended gate chemical sensitive field effect transistor as multi-species microprobe," *Sens. Actuators A, Phys.*, vol. 4, pp. 291–298, Jan. 1983.

[3] L. T. Yin, J. C. Chou, W. Y. Chung, T. P. Sun, and S. K. Hsiung, "Separate structure extended gate H^+-ion sensitive field effect transistor on a glass substrate," *Sens. Actuators B, Chem.*, vol. 71, no. 1/2, pp. 106–111, Nov. 2000.

[4] J. L. Chiang, J. C. Chou, and Y. C. Chen, "Study of the pH-ISFET and EnFET for biosensor applications," *J. Med. Biol. Eng.*, vol. 21, no. 3, pp. 135–146, 2001.

[5] N. H. Chou, J. C. Chou, T. P. Sun, and S. K. Hsiung, "Differential type solid-state urea biosensors based on ion-selective electrodes," *Sens. Actuators B, Chem.*, vol. 130, no. 1, pp. 359–366, Mar. 2008.

[6] P. D. Batista and M. Mulato, "ZnO extended-gate field-effect transistors as pH sensors," *Appl. Phys. Lett.*, vol. 87, no. 14, pp. 143508-1–143508-3, Oct. 2005.

[7] J. C. Chou, P. K. Kwan, and Z. J. Chen, " SnO_2 separative structure extended gate H^+-ion sensitive field effect transistor by the sol–gel technology and the readout circuit developed by source follower," *Jpn. J. Appl. Phys.*, vol. 42, pt. 1, no. 11, pp. 6790–6794, Nov. 2003.

[8] J. C. Chou and C. W. Chen, "Fabrication and application of ruthenium-doped titanium dioxide films as electrode material for ion-sensitive extended-gate FETs," *IEEE Sensors J.*, vol. 9, no. 3, pp. 277–284, Mar. 2009.

[9] J. C. Chou and D. J. Tzeng, "Study on the characteristics of the ruthenium oxide pH electrode," *Rare Met. Mater. Eng.*, vol. 35, no. Suppl. 3, pp. 256–258, Dec. 2006.

[10] E. M. Guerra, G. R. Silva, and M. Mulato, "Extended gate field effect transistor using V_2O_5 xerogel sensing membrane by sol–gel method," *Solid State Sci.*, vol. 11, no. 2, pp. 456–460, Feb. 2009.

[11] D. E. Yates, S. Levine, and T. W. Healy, "Site-binding model of the electrical double layer at the oxide/water interface," *J. Chem. Soc. Faraday Trans. 1*, vol. 70, pp. 1807–1818, Jan. 1974.

[12] Y. Cheng, P. Xiong, C. S. Yun, G. F. Strouse, J. P. Zheng, R. S. Yang, and Z. L. Wang, "Mechanism and optimization of pH sensing using SnO_2 nanobelt field effect transistors," *Nano Lett.*, vol. 8, no. 12, pp. 4179–4184, Dec. 2008.

[13] P. Y. Yang, J. L. Wang, P. C. Chiu, J. C. Chou, C. W. Chen, H. H. Li, and H. C. Cheng, "pH sensing characteristics of extended-gate field-effect transistor based on Al-doped ZnO nanostructures hydrothermally synthesized at low temperatures," *IEEE Electron Device Lett.*, vol. 32, no. 11, pp. 1603–1605, Nov. 2011.

[14] A. Fulati, S. M. Usman Ali, M. Riaz, G. Amin, O. Nur, and M. Willander, "Miniaturized pH sensors based on zinc oxide nanotubes/nanorods," *Sensors*, vol. 9, no. 11, pp. 8911–8923, Nov. 2009.

[15] J. L. Chiang, J. F. Hsu, S. F. Lee, L. Y. Lee, and H. Y. Liu, "Ion sensitivity of the flowerlike ZnO nanorods synthesized by the hydrothermal process," *J. Vac. Sci. Technol. B*, vol. 27, no. 3, pp. 1462–1465, May 2009.

[16] S. M. Al-Hilli, M. Willander, A. Öst, and P. Strålfors, "ZnO nanorods as an intracellular sensor for pH measurements," *J. Appl. Phys.*, vol. 102, no. 8, pp. 084304-1–084304-5, Oct. 2007.

[17] S. M. Sze, *Physics of Semiconductor Devices*, 2nd ed. New York: Wiley, 1981.